Integration of Gibbs Markov Random Field and Hopfield-Type Neural Networks for Unsupervised Change Detection in Remotely Sensed Multitemporal Images

Ashish Ghosh, *Member, IEEE*, Badri Narayan Subudhi, *Student Member, IEEE*, and Lorenzo Bruzzone, *Fellow, IEEE*

***Abstract*— In this paper, a spatiocontextual unsupervised change detection technique for multitemporal, multispectral remote sensing images is proposed. The technique uses a Gibbs Markov random field (GMRF) to model the spatial regularity between the neighboring pixels of the multitemporal difference image. The difference image is generated by change vector analysis applied to images acquired on the same geographical area at different times. The change detection problem is solved using the maximum *a posteriori* probability (MAP) estimation principle. The MAP estimator of the GMRF used to model the difference image is exponential in nature, thus a modified Hopfield type neural network (HTNN) is exploited for estimating the MAP. In the considered Hopfield type network, a single neuron is assigned to each pixel of the difference image and is assumed to be connected only to its neighbors. Initial values of the neurons are set by histogram thresholding. An expectation–maximization algorithm is used to estimate the GMRF model parameters. Experiments are carried out on three-multispectral and multitemporal remote sensing images. Results of the proposed change detection scheme are compared with those of the manual-trial-and-error technique, automatic change detection scheme based on GMRF model and iterated conditional mode algorithm, a context sensitive change detection scheme based on HTNN, the GMRF model, and a graph-cut algorithm. A comparison points out that the proposed method provides more accurate change detection maps than other methods.**

***Index Terms*— Change detection, markov random field (MRF), maximum a posteriori probability (MAP) estimation, hopfield neural network, multitemporal images, remote sensing.**

I. Introduction

THE process of detecting changes in multitemporal, multi spectral remote sensing images is fundamental in many different applications, including environmental monitoring [1], land cover dynamics [2], forest monitoring [3], geographical survey [4], urban studies [5], etc. Generally, for change detection, a pair of multitemporal images acquired on the same geographical area at different times is analyzed. The most widely used unsupervised change detection scheme includes three fundamental steps: preprocessing, comparison and analysis [6]. The preprocessing stage includes normalization of the available multitemporal remote sensing images (i.e., co-registration, radiometric correction, geometric correction, atmospheric correction, etc. [7]), so that they can be used in the subsequent stages. In the comparison step, the multispectral remotely sensed images taken over the same geographical area at different times are compared using suitable mathematical operators like, single band differencing, vector differencing, ratioing, etc. Change vector analysis (CVA) [7] based difference image generation scheme is a popular technique. In the CVA-based scheme the difference image is generated by analyzing the magnitude of the spectral change vectors obtained from vector difference of each pair of corresponding pixels.

The analysis step is aimed at producing the final change detection map. Fung and LeDrew [8] proposed a single hypothesis testing thresholding scheme for detecting changes in multispectral image data. Those pixels in the difference image having grey values significantly different from the mean of the whole image are identified as the changed pixels. Although it is an old technique, it is still in active use for different remote sensing change detection applications. An unsupervised change detection technique has been studied by Bovolo *et al.* in [9]. Here the authors presented a change detection approach that jointly analyze the spectral channels of multitemporal images in the original feature space. This is accomplished by a semi-supervised support vector machine, where a Bayesian thresholding scheme [10] is exploited for deriving an initial "pseudo" training set. All the above mentioned techniques are pixel based, and do not take into account the spatio-contextual information.

It is normally observed that information contained in a pixel in an image has a strong correlation with that of its neighboring pixels. Hence, the changes occurring at a particular location of an image are more likely to occur

Manuscript received February 3, 2010; revised March 6, 2012, May 23, 2012, and April 4, 2013; accepted April 5, 2013. Date of publication April 24, 2013; date of current version May 24, 2013. The work of B. N. Subudhi was supported by the Council of Scientific and Industrial Research, under Senior Research Fellowship 9/93 (0137)/2011. The associate editor coordinating the review of this manuscript and approving it for publication was Prof. Brian D. Rigling.

A. Ghosh and B. N. Subudhi are with the Machine Intelligence Unit, Indian Statistical Institute, Kolkata 700108, India (e-mail: ash@isical.ac.in; subudhi.badri@gmail.com).

L. Bruzzone is with the Department of Information and Communication Technology, University of Trento, Trento 38050, Italy (e-mail: lorenzo.bruzzone@ing.unitn.it).

Digital Object Identifier 10.1109/TIP.2013.2259833

in a connected region rather than at disjoint points. This indicates that a more accurate change detection map can be generated by considering context-sensitive approaches rather than context insensitive ones.

Gibb's Markov Random Field (GMRF) is a spatio-contextual statistical model mainly used for partitioning an image into a number of regions with the constraint of Gibb's distribution as prior probability distribution [11]. In GMRF, the spatial property of the image can be modeled through different aspects, among which, the contextual constraint is a general and powerful one [12]. Segmentation of an input image is obtained by estimating some spatially varying quantity from noisy measurement. This can be obtained by maximum a posteriori probability (MAP) estimate of the underlying quantity formulated in Bayesian framework [11]. The important part of GMRF model is the proper fixing of the parameters. In the literature two approaches namely, Markov chain Monte Carlo (MCMC) and expectation–maximization (EM) algorithms are used for this purpose [12]. However for its easy simulation and low complexity, EM algorithm is popularly used for many machine vision applications.

A different unsupervised change detection technique proposed by Bruzzone and Prieto [13] demonstrated the effectiveness of the GMRF model in change detection. In this technique the spatio-contextual information of pixels is modeled with a GMRF and the iterated conditional mode (ICM) algorithm is used as the MAP estimator. The GMRF model parameters are recursively estimated by the EM algorithm. ICM uses a deterministic strategy to find the local minimum. It starts with an initial estimate and for each pixel, the cluster centre that results in decrease in energy is chosen for the next iteration. Hence the results provided by ICM are extremely sensitive to the initial estimate, and it may stuck in local minima.

In [14], Ghosh *et al.* have proposed an object background separation scheme using GMRF model as the *a priori* image model and used Hopfield type network [15] for MAP estimation. This work shows that Hopfield type neural network (HTNN) can be used for performing a fast and approximate optimization like deterministic ICM algorithm [15]. The optimization function can be mapped to correspond to the energy function of an HTNN. When the network converges to a stable state, its energy value corresponds to a minimum of the optimization function. It is also observed that the stochastic nature of the network helps to avoid getting trapped in a local minimum and improves the quality of solution, thus producing better solutions than the ICM algorithm [12].

Recently, an unsupervised change detection technique is proposed by Bazi *et al.* [16] using level set scheme. Here the change detection problem is considered as a binary segmentation of the difference image into the changed and the unchanged classes by defining a proper energy functional. This energy function is minimized by level set. Use of kernel based methodologies for unsupervised change detection are quite popular these days. A non-linear kernel based classifier is proposed by Camps-Valls *et al.* [17] for detecting changes from multitemporal remote sensing images. The integration of contextual information and multi-sensor images with different levels of nonlinear sophistication gives better accuracy in change detection. However, this approach is affected by the curse-of-dimensionality problem and hence requires large computation. A spatio-contextual change detection scheme is also reported in [6], where HTNN is used to detect the changed region corresponding to multitemporal remote sensing images. It is found that HTNN updates the output status of the neurons until a minimum of the energy function is reached. However, in [6] the correlation between the pixels of the difference image are expressed in a deterministic way. To the best of the authors' knowledge, use of both these approaches (i.e., EM algorithm with GMRF modeling and HTNN) was not addressed in remote sensing change detection literature.

In this article, we present a technique that exploits the EM algorithm with GMRF modeling and HTNN for MAP estimation to detect the changes in multitemporal, multi spectral remote sensing images. The proposed unsupervised change detection scheme uses the GMRF model as the *a priori* difference image model. The problem of change detection is considered as a two class pixel labeling problem and is formulated as a MAP estimation problem. Since the MAP estimate of the GMRF modeled difference image is computationally expensive, a modified version of HTNN is used to solve it. Here we have considered each pixel of the difference image as a neuron connected to its neighbors. Since the change detection problem is considered as a MAP estimation problem of the GMRF modeled difference image with an HTNN, an equivalence between the expression of MAP of GMRF model and the energy function of an HTNN is established. Then an iterative updating rule is provided so that convergence of the network is guaranteed. We used an EM algorithm to estimate the parameters of GMRF and the network is initialized by using an automatic threshold selection scheme based on Liu's [18] histogram thresholding algorithm. To show the effectiveness of the proposed technique, results are compared with those provided by manual trial and error thresholding (MTET), change detection scheme based on the GMRF model and the ICM algorithm [13], change detection scheme based on HTNN [6], and change detection scheme using the GMRF model and graph-cut algorithm [19]. It is found that the proposed scheme gives more reliable change detection results than the other techniques.

The organization of this paper is as follows. Section II presents an overview of the proposed technique. Section III provides a brief description of the GMRF modeling and GMRF-MAP framework. Section IV provides a description of the developed HTNN and MAP estimation process. The data sets used in our experiments and the corresponding change detection results are analyzed in Section V. Finally, Section VI draws the conclusions of this work.

II. Proposed Technique for Change Detection

A block diagram of the proposed technique is given in Fig. 1. The first part of the block diagram represents f_1 and f_2 to be two co-registered and radiometrically corrected γ-spectral band images of size $M \times N$, acquired over the same geographical area at two times T_1 and T_2. In the first step of processing the CVA scheme [7] is used to generate the difference image according to the magnitude of the

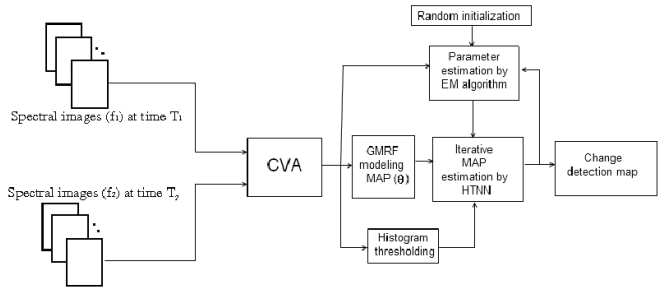

Fig. 1. Block diagram of the proposed change detection technique.

spectral change vectors. By classifying this difference image into changed and unchanged classes it is possible to obtain the change detection map of the considered area. To classify the difference image into two classes, we propose the use of GMRF based probabilistic modeling and HTNN as MAP estimator. The use of the GMRF probabilistic model gives an advantage of approximating the spatial regularities of pixels (see the "GMRF modeling MAP (θ)" block in Fig. 1). Here the MAP estimation of the GMRF modeled difference image is obtained by a modified HTNN. Since the estimation of GMRF model parameters using EM algorithm is well studied in the literature [12], [13], we have used such an algorithm to iteratively estimate these parameters (see the "parameter estimation by EM algorithm" block in Fig. 1). The Hopfield network [15] is initialized by thresholding the input image based on Liu's [18] threshold selection algorithm. The MAP estimated image is a map of two classes i.e., changed and unchanged.

III. Difference Image Modeling and MAP Estimation

Let y be the difference image associated with the magnitude of spectral change vectors obtained by the CVA technique [7]. We assume here that the observed difference image y is a spatial entity of size $S = M \times N$. Each pixel in y is assumed as a site s denoted by y_s, $s \in S$, where S represents the complete image. Let Y represent a random field and y be a realization of it. Let X be a random variable taking value "+1" or "−1". A realization of $X = x$ is a partitioning of the image into two region types i.e., changed (+1) and unchanged (−1). Each region type can occur in more than one physical location in the image.

Here we used a second order GMRF modeling in the spatial dimension. It is known [12] that if X is a GMRF, then it satisfies the Markovianity property in the spatial dimension

$$P(X_s = x_s \mid X_q = x_q, \forall q \in S, s \neq q) = P(X_s = x_s \mid X_q = x_q, q \in \eta_s);$$

where η_s denotes the neighborhood of s. In the spatial domain, X represents the GMRF model of x. According to Hammersley Clifford theorem [12] the prior probability at a particular temperature T can be expressed as Gibbs distribution with $P(X = x) = \frac{1}{z} e^{\frac{-\bar{U}(x)}{T}}$. Here z represents the partition function expressed as $z = \sum_x e^{\frac{-\bar{U}(x)}{T}}$, and $\bar{U}(x)$ is the energy function (a function of clique potentials $V_c(x)$). For clique c coming from the set of cliques C, the expression for $V_c(x)$ can be given as

$$\bar{U}(x) = \sum_{c \in C} V_c(x). \tag{1}$$

The change detection problem is considered to be a process of determining the realization x that has given rise to the actual noisy difference image y. The realization x can not be obtained deterministically from y. Hence, $\hat{x}$ should be estimated from y. One way to estimate $\hat{x}$ is based on the statistical MAP criterion. The objective in this case is to have an estimation rule which yields $\hat{x}$ that maximizes the following posterior probability distribution

$$\hat{x} = \arg \max_x \frac{P_\theta(Y = y|X = x)P(X = x)}{P(Y = y)}, \tag{2}$$

where θ is the parameter vector associated with x. Here y is known and the marginal probability $P(Y = y)$ is constant and can be discarded. As X is supposed to be a GMRF, its probability of realization is expressed as

$$P(X = x) = \frac{1}{z} e^{-\bar{U}(x)} = \frac{1}{z} e^{[-\sum_{c \in C} V_c(x)]}. \tag{3}$$

In (3), $V_c(x)$ is the clique potential function and is a function of the MRF model bonding parameter β and can be expressed as $V_c(x) = \beta \bar{I}(s, q)$. Choice of parameter β controls the smoothness of segmentation. A larger value of β imposes a larger penalty for inhomogeneity. As the value of β increases, the degree of smoothness imposed on the segmentation also increases. $\bar{I}(s, q)$ is a function defined over the neighbors of each site s as

$$\bar{I}(s, q) = \begin{cases} -1 \text{ if } x_s \neq x_q \text{ and } q \in \eta_s \\ +1 \text{ if } x_s = x_q \text{ and } q \in \eta_s. \end{cases}$$

The likelihood function $P_\theta(Y = y|X = x)$ models the conditional dependence and is considered to be Gaussian distributed $N(\mu_l, \sigma_l^2)$. Each class (l) can be represented by its mean vector μ_l and variance σ_l^2. Thus, the likelihood function can be expressed as

$$N(\mu_l, \sigma_l^2) = \frac{1}{\sqrt{(2\pi)\sigma_l^2}} e^{-\frac{1}{2\sigma_l^2}\|y - \mu_l\|^2}. \tag{4}$$

It may be noted that pixel gray value at each site is assumed to be independent. This yields the following simplified form of the likelihood function

$$P_\theta(Y = y|X = x) = \prod_{s \in S} P_\theta(Y_s = y_s|X_s = l) = \prod_{s \in S} \frac{1}{\sqrt{(2\pi)\sigma_l^2}} e^{-\frac{1}{2\sigma_l^2}\|y_s - \mu_l\|^2}. \tag{5}$$

In (5), variance $\sigma_l^2 \in \{\sigma_c^2, \sigma_u^2\}$ represents the variance corresponding to the changed and the unchanged classes. Similarly, $\mu_l \in \{\mu_c, \mu_u\}$ represents the mean corresponding to the changed and the unchanged classes. Considering the prior probability of GMRF and the likelihood function as in (5),

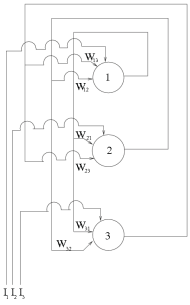

Fig. 2. Hopfield's neural network with three neurons.

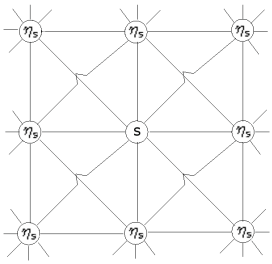

Fig. 3. Second-order topology of a network. Each neuron in the network is connected to its eight neighbors. Neurons: circles and lines: connections between neurons.

we can deduce from (2)

$$\hat{x} = \arg \max_{x} \sum_{s \in S} \left\{ A - \left[\frac{\|y_s - \mu_l\|^2}{2\sigma_l^2} \right] \right\} - \left[\sum_{c \in C} V_c(x) \right], \tag{6}$$

where $A = -\sum_{s \in S} \frac{S}{2} \log(2\pi\sigma_l^2)$ is a constant and $\hat{x}$ is the MAP estimate. Calculation of $Y|X$, and $X|Y$ depends on θ. Maximization of (6) requires 2^{bS} possible image configurations to be searched, where b represents the number of bits required to represent the segmented image. As we are performing a binary segmentation (either changed or unchanged class) each pixel can be represented as "+1" or "−1", hence $b = 1$. We used an HTNN to obtain the final MAP estimate. In the considered GMRF framework θ corresponds to five parameters i.e., $\theta = \{\beta, \mu_c, \mu_u, \sigma_c^2, \sigma_u^2\}$. We have estimated these parameters by the EM algorithm [12].

IV. Hopfield Type Neural Network for MAP Estimation

Hopfield's neural network is a physical system in the state space having a number of locally stable states. It can be regarded as an associative memory or content addressable memory [15]. Hopfield's network consists of a set of neurons or nodes. The output of each neuron (or node) is given as input to other neurons to which it is connected as shown in Fig. 2. In Hopfield's network, at any iteration of processing (time t) the input U_s^t to the generic s^{th} neuron is the sum of two quantities: the external input bias I_s (a fixed bias applied externally to the unit s) and the output of other neuron v_q^{t-1} multiplied with weight W_{sq}^{t-1}. This can be described as

$$U_s^t = \sum_{q=1, q \neq s}^{r} W_{sq}^{t-1} v_q^{t-1} + I_s. \tag{7}$$

The synaptic weights connecting two neurons are symmetric in nature, i.e., $W_{sq}^{t-1} = W_{qs}^{t-1}$.

In this model the activation function is assumed to be continuous and monotonically non-decreasing in nature. The output v_s^t of any neuron (which in turn determines the new state of the network) s is defined as

$$v_s^t = g(U_s^t), \tag{8}$$

where $g(.)$ is an activation function. A typical choice of g can be given as

$$g(U_s^t) = \frac{2}{1 + e^{-(U_s^t - \lambda)/\lambda_0}} - 1. \tag{9}$$

Here the parameter λ controls the shifting of the function g along x axis and λ_0 determines the steepness of the curve. The energy function of this architecture is given by

$$E(v^t) = -\sum_{s=1}^{r} \sum_{q=1, q \neq s}^{r} W_{sq}^t v_s^t v_q^t - \sum_{s=1}^{r} I_s v_s^t + \sum_{s=1}^{r} \frac{1}{R_s} \int_0^{v_s^t} g^{-1}(u) du. \tag{10}$$

Here $E(v^t)$ is a Lyapunov function, R_s is the input impedance of the amplifier realizing the neuron and $v^t = \{v_1^t, v_2^t, \ldots, v_r^t\}$. r represents the total number of neurons.

In this article we used a modified version of Hopfield's original network [15]. Here each neuron is assumed to be connected to its neighbors only. Hence the connection strength outside the neighborhood is assumed to be zero. Since in the present work a modified version of the Hopfield neural network is considered, it is termed as HTNN.

To detect changed and unchanged pixels from the difference image, we initially modeled the difference image with a GMRF. The spatio-contextual modeling of the difference image is obtained by formulating Gibbs distribution over each site s of the difference image. Then for MAP estimation of the GMRF modeled difference image we used an HTNN. For the considered network, each site s of the difference image is assumed to have a neuron. Each neuron is assumed to be connected with its neighbors in the spatial dimension with a connection strength of W_{sq}^t. The neuron at any position is connected to its d^{th} order neighbors included in N^d. Here, a second order neighborhood system has been considered, i.e., $N_2 = (\pm 1, 0), (0, \pm 1), (1, \pm 1), (-1, \pm 1)$. Fig. 3 depicts a second order (N_2) topological network.

It is found from (8) and (9) that for any point s

$$v_s^t = \lim_{U_s^t \to \infty} g(U_s^t) = +1, \text{ and}$$
$$v_s^t = \lim_{U_s^t \to -\infty} g(U_s^t) = -1.$$

In this work, we used a generalized fuzzy S-function [20] as activation function and is defined as follows [6]

$$v_s^t = g(U_s^t) = \begin{cases} -1, & \text{if} \quad U_s^t \le a \\ 2^n \left(\frac{U_s^t - a}{c-a}\right)^n - 1, & \text{if } a \le U_s^t \le b \\ 1 - 2^n \left(\frac{U_s^t - a}{c-a}\right)^n, & \text{if } a \le U_s^t \le b \\ 1, & \text{if} \quad U_s^t \ge c, \end{cases} \tag{11}$$

for n (an integer) ≥ 2 and $b = (a+c)/2$. Here a, b, c are real numbers and $a < b < c$. $g(U_s^t)$ lies in the range $[-1, +1]$ with $g(U_s^t) = 0.0$ at $U_s^t = b$. n can be varied to control the steepness of the curve. In the present case, as we used 8 neighbors of a site, the input will lie in the range $[-8, +8]$. However, for quick convergence we have used the domain of U_s^t as $[-1, +1]$ and used the activation function as

$$v_s^t = g(U_s^t) = \begin{cases} -1, & \text{if} \quad U_s^t \le -1 \\ \left(U_s^t + 1\right)^n - 1, & \text{if } -1 \le U_s^t \le 0 \\ 1 - \left(1 - U_s^t\right)^n, & \text{if } \ 0 \le U_s^t \le 1 \\ 1, & \text{if} \quad U_s^t \ge 1. \end{cases} \tag{12}$$

A. Solving the MAP Estimation Problem With Hopfield Type Neural Network

HTNN is a robust and fast optimization technique. Unlike the ICM algorithm which can be seen as a local search algorithm, the stochastic nature of the HTNN helps to avoid getting trapped to a local optimum. Thus it may improve the quality of solution (and therefore of the change detection map) with respect to the ICM algorithm. In HTNN, a proper initialization is necessary to start the iterative process. In GMRF-MAP estimation the algorithm starts with an initial estimate and then converges to a minimum of the cost function.

As stated previously, in the proposed scheme the MAP estimation problem is considered as a two class pixel labeling problem. The labels obtained for the pixels of the difference image framework generate regions corresponding to the changed and unchanged classes. Hence we have assumed the final labels as $+1$ and -1. For the sake of simplicity, in this work we will confine ourselves to cliques with two pixels only [12].

As the change detection problem is viewed as a MAP estimation problem of the GMRF modeled difference image with HTNN, it suffices to establish an equivalence between (6) and the energy of an HTNN, and to provide an updating rule so that convergence is guaranteed. The clique potential function $V_c^t(x)$ in (6) is defined as

$$V_c^t(x) = -W_{sq}^t v_s^t v_q^t, \tag{13}$$

where v_s^t and v_q^t represent the output of the s^{th} and q^{th} neurons, respectively and W_{sq}^t is the connection weight between them. Value of connection strengths are computed as

$$W_{sq}^t = \beta \bar{I}^t(s,q), \tag{14}$$

where β is a parameter associated with the clique potential function and is a GMRF model parameter. $\bar{I}^t(s,q)$ is a function defined over the neighbors of each site as

$$\bar{I}^t(s,q) = \begin{cases} -1 \text{ if } x_s^t \ne x_q^t \text{ and } q \in \eta_s \\ +1 \text{ if } x_s^t = x_q^t \text{ and } q \in \eta_s. \end{cases}$$

Substituting (14) in (13) we get

$$V_c^t(x) = -\beta \bar{I}^t(s,q) v_s^t v_q^t.$$

To some extent, this potential function resembles the Potts model i.e., a generalization of Ising model [12]. Hence (3) can be re-written as

$$P(X = x) = \frac{1}{z} e^{\left[-\sum_{c \in C} -\beta \bar{I}^t(s,q) v_s^t v_q^t\right]}. \tag{15}$$

For implementing the GMRF model with Hopfield's network we may interpret y as the initialization of the network (each site/pixel is considered as a neuron). Similarly μ_l can be interpreted as the present state of the network. Thus we may rewrite (6) as

$$\hat{x} = \arg \max_x \left\{ A - \frac{\sum_s (I_s - v_s^t)^2}{2\sigma^2} + \sum_{(s,q), s \ne q} W_{sq}^t v_s^t v_q^t \right\}.$$

Maximization of above expression is equivalent to minimization of

$$\hat{x} = \arg\min_x \left\{ \left[\frac{1}{2\sigma^2} \sum_s (v_s^t)^2 \right] - \left[\frac{1}{\sigma^2} \sum_s I_s v_s^t \right] - \left[\sum_{(s,q), s \ne q} \mathrm{W}_{\mathrm{sq}}^{\mathrm{t}} v_s^t v_q^t \right] \right\}. \tag{16}$$

Now the problem is reduced to the minimization of (16). We can establish an equivalence between (16) and the energy function in (10) and provide an updating rule so that convergence is guaranteed. Comparing (10) and (16), one can see that the standard Hopfield's network cannot be used for minimization of (16) due to the presence of the extra term $\frac{1}{2\sigma^2} \sum_s (v_s^t)^2$. In order to realize (16) with a network we used an HTNN as used in [14] whose energy function can be described as

$$E(v^t) = -\sum_{s=1}^{r} \sum_{q=1, q \ne s}^{r} W_{sq}^t v_s^t v_q^t - \sum_{s=1}^{r} I_s v_q^t + \frac{1}{2R} \sum_{s=1}^{r} (v_s^t)^2 + \sum_{s=1}^{r} \frac{1}{R_s} \int_0^{v_s^t} g^{-1}(u) du, \tag{17}$$

and

$$\frac{dE(v^t)}{dt} = -\sum_s \left\{ k (g^{-1})' \right\} \left(\frac{dv_s^t}{dt} \right)^2, \tag{18}$$

where, k is a positive constant. It can be easily shown [14] that for any monotonic increasing function g, the expression $\frac{dE}{dt} \le 0$, and $\frac{dE}{dt} = 0 \Rightarrow \frac{dv_s^t}{dt} = 0$. Hence, searching in the gradient direction will reach the minimum of E. The last term in (17) is the energy loss term. In the high gain limit the last term can be excluded and thus (17) can be written as

$$E(v^t) = \sum_{s=1}^{r} \left[-\sum_{q=1, q \ne s}^{r} W_{sq}^t v_s^t v_q^t - I_s v_s^t + \frac{1}{2R} (v_s^t)^2 \right]. \tag{19}$$

By proper adjustment of coefficients, (16) can be made equivalent to minimize $E(v^t)$.

Here we have considered $\theta = \{\beta, \mu_c, \mu_u, \sigma_c^2, \sigma_u^2\}$ as the parameter vector associated with the probability density function (pdf) of the incomplete data y. The parameter vector θ is estimated recursively in the EM framework [12].

It may be noted that in [6] a deterministic way of specifying the correlation of pixels of the difference image was used. The synaptic weights corresponding to two neurons of the neural network were considered as $W_{sq}^t = W_{qs}^t = 1$. On the contrary, in the proposed scheme we have modeled the difference image with GMRF and thus a modified form of connection weight is considered. In addition, in the proposed work we used the expression in (16), through the equivalence of the energy expression of the HTNN in (19), for estimating the MAP of the GMRF modeled difference image (as expressed in (6)). Contrarily, in [6] the energy function corresponding to Hopfield's network as specified in (10) was used for change detection in multitemporal images. Hence, the proposed scheme uses an HTNN in a different and new way for change detection of remote sensing images.

B. Network Initialization

In literature, initialization of each neuron of the HTNN is carried out by considering a linear transfer function [14] (see the thin line in Fig. 4)

$$I_s = \frac{y_s}{(L/2)} - 1,$$

where y_s represents the input pixel value, L the maximum pixel value of the image and I_i the input bias to the i^{th} neuron. This function is symmetric about the point $L/2$ (called initialization threshold). The pixels having value below $L/2$ are transformed to a negative quantity in the range $[-1, 0)$ and the pixels having value above $L/2$ are transformed to a positive quantity in $[0, +1]$. Such kind of transfer function was considered by authors in [14], where the grey values of the image pixels were expected to cover the entire range $(0, L)$. In our work, we used noise corrupted remotely sensed images whose grey values do not cover the entire dynamic range. Hence the use of such a transfer function for initialization may not give satisfactory results. Again consideration of $L/2$ as the initialization threshold has no resemblance with the optimal threshold value. Hence, we used an automatic threshold selection scheme capable of giving satisfactory results in this context.

Fig. 4 represents two curves, one is a linear function as used in [14] and the other is a piece-wise linear function. In the present work we used the piece-wise linear transfer function. This curve passes through the x-axis at a value Th defined as

$$I_s = \begin{cases} \dfrac{y_s}{Th} - 1, \text{ if } -1 \le \left(\dfrac{y_s}{Th} - 1\right) \le +1 \\ +1, \text{ if } \quad \left(\dfrac{y_s}{Th} - 1\right) \ge 1. \end{cases} \tag{20}$$

To have an estimate of Th, we have used Liu's thresholding scheme [18].

V. Results and Analysis

In order to establish the effectiveness of the proposed technique, we have tested it on three data sets related to Mexico, Sardinia island (Italy) and Peloponnesian Peninsula (Greece). In order to validate the proposed technique, we have compared its results with those obtained by: (i) the MTET, (ii) a change detection scheme based on GMRF model and ICM algorithm [13], (iii) the HTNN presented in [6], and (iv) the change detection scheme based on GMRF model and graph-cut algorithm [19]. All the results reported in the proposed article, are based on the absolute pixel counts. For remote sensing change detection, measures like missed alarms, false alarms and overall error as performance evaluation criteria are largely reported in the literature. Hence to establish the effectiveness of the proposed scheme, we also used those performance criteria for evaluation.

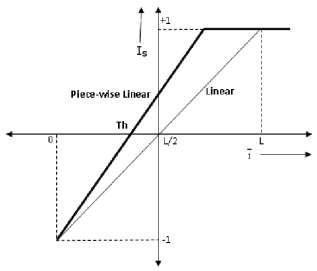

Fig. 4. Initial bias to Hopfield type neural network.

The Manual trial and error technique (MTET) is one of the simplest ways to perform the change detection task. MTET produces a minimum error change detection map by manually finding decision threshold on the difference image under the assumption that pixels are independent in the spatial domain. The minimum error decision threshold is obtained in a supervised way by computing the change detection error (with the help of a ground-truth map) for all values of the decision threshold [21].

We analyzed the overall change detection error, missed and false alarms. The missed alarms and the false alarms are obtained by pixel by pixel comparison of the obtained change detection map with the available reference change detection map. Missed alarms are obtained by computing the number of pixels that actually belong to changed regions and are found to belong to unchanged regions. The false alarms are obtained by computing the number of pixels that actually belong to the unchanged regions and are found to belong to the changed regions.

1) Mexico Data Set: The first data set used in our experiments is made up of two multispectral images acquired by the Landsat Thematic Mapper (TM) sensor of the Landsat-7 satellite in an area of Mexico in April 2000 and May 2002. From the entire available Landsat scene, a section of 512×512 pixels has been selected as test site. Fig. 5(a) and (b) show channel 4 of the 2000 and 2002 images, respectively. Between the two aforementioned acquisition dates, fire destroyed a large portion of the vegetation in the considered region.

To make a quantitative evaluation of the effectiveness of the proposed approach, a reference map was manually defined [see Fig. 5(d)] according to a detailed visual analysis of both the available multitemporal images and the difference image [see Fig. 5(c)] [6]. Details of the preprocessing done on the image can be found in [6].

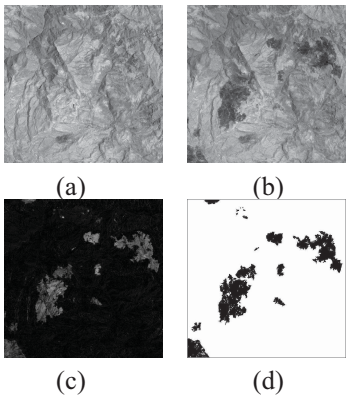

Fig. 5. Mexico data set: band 4 of the Landsat TM image acquired in (a) April 2000, (b) May 2002, (c) corresponding difference image generated by the CVA technique, and (d) reference map of the changed area.

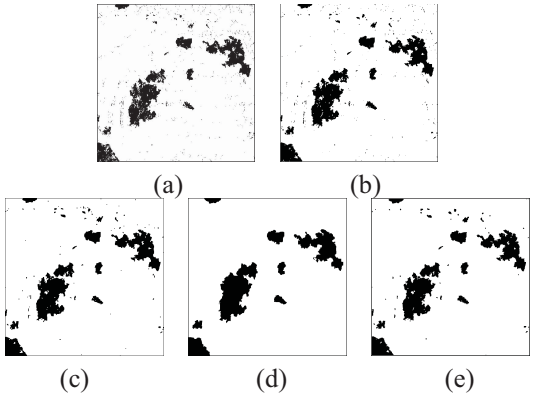

Fig. 6. Mexico data set: change detection maps provided by (a) MTET, (b) GMRF model and ICM algorithm, (c) Context sensitive Hopfield type network, (d) GMRF model and graph-cut algorithm, and (e) Proposed technique.

The threshold value obtained for the difference image obtained by CVA technique was 39 using Liu's thresholding scheme [18]. Putting this threshold value in (20), an initial bias is obtained. The parameters of the GMRF model were initially set to some random values. The MAP estimation of the difference image was obtained by an HTNN with initial bias determined by the above threshold. The EM algorithm was used to estimate the GMRF model parameters. The change detection map obtained by the proposed technique for Mexico data set is displayed in Fig. 6(e). This map corresponds to an overall change detection error of 2380 pixels with 388 missed alarms and 1992 false alarms.

The change detection results obtained by the proposed approach are compared with those yielded by other reference techniques. The change detection map obtained by MTET scheme is displayed in Fig. 6(a). As expected, the proposed technique is more accurate than the MTET, thanks to the use of the contextual information. The change detection map obtained by GMRF model and ICM algorithm is shown in Fig. 6(b). Similarly, the change detection map obtained by HTNN model is provided in Fig. 6(c) (with initialization threshold $Th = 31$). The change detection maps obtained by the GMRF model and graph-cut algorithm is shown in Fig. 6(d). It provided a smooth change detection map. Table I

TABLE I
OVERALL ERROR, MISSED ALARMS, AND FALSE ALARMS RESULTING FROM DIFFERENT TECHNIQUES FOR MEXICO DATA SET

Technique	Missed Alarms	False Alarms	Overall Error
MTET (Th=39)	2404	2187	4591
EM+GMRF+ICM	946	2257	3203
HTNN (Th=31)	660	2157	2817
GMRF+Graph-cut	636	2643	3279
Proposed (Th=37)	388	1992	**2380**
Proposed (Avg β)	588	1850	2438

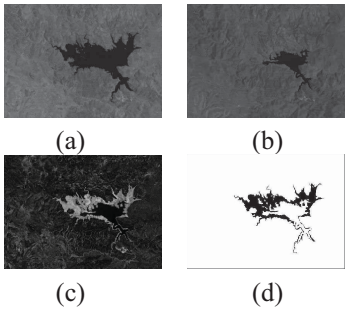

Fig. 7. Sardinia Island (Italy) data set: band 4 of the Landsat TM image acquired in (a) September 1995, (b) July 1996. (c) Difference image generated by the CVA technique using bands 1, 2, 4, and 5, and (d) reference map of the changed area.

shows a comparison of errors provided by different techniques. The analysis in Table I confirms that the proposed technique provided the lowest change detection error on this data set. Please note that we need initial threshold values for MTET, HTNN and the proposed scheme. However, the GMRF+ICM and GMRF+graph-cut approaches use initial mean values corresponding to different clusters (randomly).

2) Sardinia Island Data Set: The second data set used in our experiments is made up of two multispectral images acquired by the Landsat TM sensor of the Landsat-5 satellite in September 1995 and July 1996. The test site is a section (412×300 pixels) of a scene including Lake Mulargia on the Island of Sardinia (Italy). Between the two aforementioned acquisition dates, the water level in the lake increased (see the lower central part of the image). Fig. 7(a) and (b) show channel 4 of the 1995 and 1996 images, respectively. As done for the Mexico data set, also in this case, a reference map was manually defined [see Fig. 7(d)] according to a detailed visual analysis of both the available multitemporal images and the difference image [see Fig. 7(c)] [22]. Details on the preprocessing of the image can be found in [6]. We applied the CVA technique to spectral bands 1, 2, 4, and 5 of the two multispectral images, as preliminary experiments showed that the above channels contain useful information on the changes in the water level [6].

As for the Mexico data set, we also determined the threshold value of the difference image for initialization of the HTNN. The threshold value obtained by Liu's method is 85. The change detection map obtained by the proposed technique is shown in Fig. 8(e). It is associated with a change detection error of 1496 pixels with 845 missed alarms and 651 false alarms.

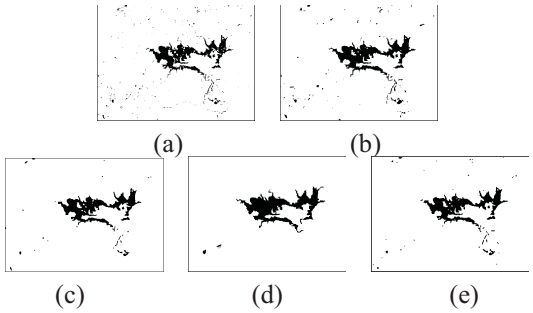

Fig. 8. Sardinia Island (Italy) data set: change detection map provided by (a) MTET, (b) GMRF model and ICM algorithm, (c) Context sensitive Hopfield type network, (d) GMRF model and graph-cut algorithm, and (e) Proposed technique.

TABLE II
OVERALL ERROR, MISSED ALARMS, AND FALSE ALARMS RESULTING FROM DIFFERENT TECHNIQUES FOR SARDINIA ISLAND DATA SET

Technique	Missed Alarms	False Alarms	Overall Error
MTET (Th = 95)	1015	875	1890
EM+GMRF+ICM	592	1108	1700
HTNN (Th = 87)	1193	606	1799
GMRF+Graph-cut	1093	477	1570
Proposed (Th = 86)	845	651	**1496**
Proposed (Avg β)	814	688	1502

We also compared the change detected output of Sardinia Island data with other three reference methods. The change detection map obtained by the MTET and GMRF model with ICM algorithm are shown in Fig. 8(a) and (b). It is observed that both the techniques have produced a large number of false alarms. Similarly, the change detection map obtained by the context sensitive HTNN scheme (with initialization threshold $Th = 90$) and GMRF model with graph-cut scheme are shown in Fig. 8(c) and (d), which are found to be providing smooth change detection maps. A comparison of change detection errors produced by all these techniques are provided in Table II. It is observed from these results that the proposed technique provided the minimum overall error.

3) Peloponnesian Peninsula Data Set: The third data set used in the experiments was acquired by the multispectral Wide Field Sensor (WiFS) mounted on board the IRS-P3 satellite. The area considered is a section (492×492 pixels) of a scene acquired in the southern part of the Peloponnesian Peninsula, Greece, in April 1998 and September 1998. Fig. 9(a) and (b) show channel 2 [i.e., near-infrared spectral (NIR) channel] of images of April and September, respectively. A Wildfire destroyed a significant portion of the vegetation in the aforesaid area between the two dates. As for the previous two data sets, in this case also a reference map was manually defined (see Fig. 9(d)) to assess change detection errors. This reference map contains 5197 changed and 236 867 unchanged pixels. For preprocessing on this data set we refer the reader to [22].

In this case, the difference image is generated by using only NIR band images, as NIR band is very effective to locate the burned area.

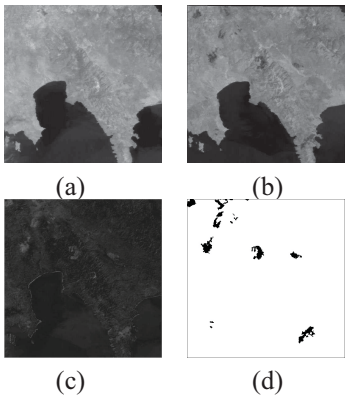

Fig. 9. Peloponnesian Peninsula (Greece) data set: NIR band of the IRS-P3 WiFS image acquired in (a) April 1998, (b) September 1998. (c) Corresponding difference image generated by CVA technique using the NIR band; and (d) Reference map of the changed area.

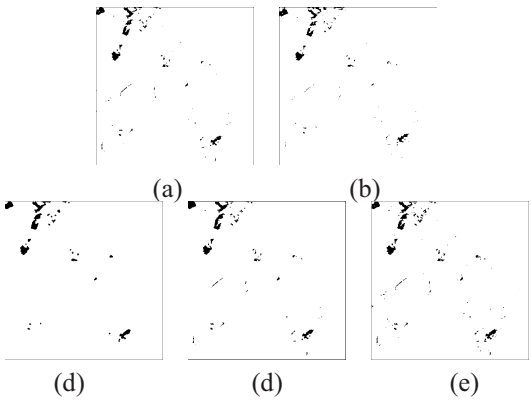

Fig. 10. Peloponnesian Peninsula (Greece) data: change detection map provided by (a) MTET, (b) GMRF model and ICM algorithm, (c) Context sensitive Hopfield type network, (d) GMRF model and graph-cut algorithm, and (e) Proposed technique.

TABLE III
OVERALL ERROR, MISSED ALARMS, AND FALSE ALARMS RESULTING FROM DIFFERENT TECHNIQUES FOR PELOPONNESIAN PENINSULA (GREECE) DATA SET

Technique	Missed Alarms	False Alarms	Overall Error
MTET (Th = 64)	2424	1129	3553
EM+GMRF + ICM	1837	1072	2909
HTNN (Th = 57)	1888	920	2808
GMRF+Graph-cut	1983	840	2823
Proposed (Th = 55)	1725	1027	2752
Proposed (Avg β)	1910	831	**2741**

The threshold value obtained for the difference image of this data set using Liu's algorithm is 55. Using 55 as the initialization threshold for the HTNN, the MAP estimate of the GMRF modeled difference image is obtained. The change detection map provided by the proposed technique is shown in Fig. 10(d). This results in an overall error of 2752 pixels, with 1725 missed alarms and 1027 false alarms.

Also in this case we compared the change detection maps obtained by the proposed technique with the maps obtained by reference techniques. The change detection maps obtained by

MTET, GMRF model with ICM algorithm, HTNN scheme and GMRF model with graph-cut scheme are shown in Fig. 10(a)–(d). Table III gives a comparison of all results produced by different techniques on this data set. Also in this case the proposed technique resulted in the minimum overall error, even its performance is similar to that of the other two context sensitive techniques. In the considered work we found that the actual estimation of GMRF model bonding parameter (β) is a critical issue. Different values of β converge to different solutions (i.e., different change detection maps).

A. Discussion

MTET, the GMRF model and ICM based Experiments carried out on the considered multitemporal remote sensing data sets pointed out that the proposed technique produces better results than the other reference techniques. This mainly depends on the stochastic nature of the HTNN that helps to avoid getting trapped to local optima and improves the quality of solution with respect to the ICM algorithm. The change detection maps obtained by the presented technique are smoother than those generated by MTET, MRF-ICM, and HTNN schemes. Sometimes it happens that a small unchanged region surrounded by a large changed region is incorrectly identified as changed region (and vice versa). However, it does not erode small scale changes completely. A manual fixing of the GMRF model bonding parameter (β) can control this.

The results reported in the previous sections were obtained by the optimal (!) value of β according to preliminary experiments. Although β can be defined taking into account the densed inference of the contextual information in the change detection map, in real scenarios its choice can be critical. To better access the effects of β on the change detection results, we experimented with five different random initialization values of β in the range [0, 3]. Then we computed the average errors for three different images. It is found that the average overall change detection error is very close to the best change detection results as depicted in Tables I, II, III, respectively. From the above analysis we experienced that choice of parameter β is critical for change detection. Smaller regions with detailed boundary can be obtained by proper fixing of parameter β with affordable false alarms. Hence, fixing of parameter β is a critical issue. In this regards we suggest that some adaptive model-based approaches which follow local pdf of the difference image may be considered for automatic estimation of parameter β.

It may be noted that for any noisy or less illuminated scene it is observed that MTET scheme always provides biased results. However this is improved in case of MRF based and HTNN based schemes. GMRF and ICM scheme can discriminate the noise by proper fixing of the beta parameter; but will provide smoother border with missing details. For the considered datasets we found that the results obtained by the GMRF + ICM are not better than the proposed scheme. We also tested the GMRF + ICM with other parameter values and the results are found to be worse than those reported in [6], [13] and [22]. GMRF model with graph cut is able to cope with this. However, it is not able to detect small regions and irregular boundary details of a scenes. Hence, it provides more missed alarms. The results obtained by HTNN scheme is able to provide better results from the noisy scene by removing irrelevant details and is found to provide smooth results. This was performed by fixing the weights of the HTNN, where weights are considered to be unit. In the proposed scheme the variation of the beta value controls this and for irregular boundaries it needs a small beta value, whereas for smoother boundary, beta value is required to be high with affordable amount of loss.

VI. Conclusion and Future Works

In this paper an unsupervised spatio-contextual change detection technique for multitemporal, multi spectral remote sensing images has been proposed. Initially, a difference image is generated by comparing the images acquired over the same geographical area at different times by CVA. The difference image is modeled with the well known GMRF model and the corresponding labels are estimated using the MAP estimation criterion. As the computation of MAP is exponential in nature, we have used a modified version of Hopfield's neural network to estimate the MAP of the GMRF model. EM algorithm is used to estimate the GMRF model parameters.

We have carried out experiments on three multispectral and multitemporal remote sensing images and the results are found to be good. To show the effectiveness of the proposed technique, results are compared with those of MTET, change detection scheme based on the GMRF model and the ICM algorithm, change detection scheme based on HTNN, and change detection scheme using the GMRF model and graph-cut algorithm. It is found that the proposed scheme gives more reliable change detection results than other techniques.

In this paper we have formulated the MAP estimation under the assumption that the prior probability follows Gibbs distribution (multilevel logistic model). As the change detection map usually has spatial regularity or region continuity, it is expected that the use of a Gauss MRF model may also provide better change detection output. In this article we have presented all the results considering it as a two class segmentation task. However it can be extended for multi-class segmentation problem by considering the multiple stability analysis of the HTNN network. The use of CVA for difference image generation is very popular in remote sensing literature. However, difference image with spectral features is expected to produce good results. In our future work we would like to focus on this issue.

References

[1] P. S. Chavez and D. J. MacKinnon, "Automatic detection of vegetation changes in the southwestern united states using remotely sensed images," *Photogram. Eng. Remote Sens.*, vol. 60, no. 5, pp. 1285–1294, 1994.

[2] R. S. Lunetta, J. F. Knight, J. Ediriwickrema, J. G. Lyon, and L. Dorsey Worthy, "Land-cover change detection using multi-temporal MODIS NDVI data," *Remote Sens. Environ.*, vol. 105, no. 2, pp. 142–154, Nov. 2006.

[3] S. Gopal and C. Woodcock, "Remote Sensing of forest change using artificial neural networks," *IEEE Trans. Geosci. Remote Sens.*, vol. 34, no. 2, pp. 398–404, Mar. 1996.

[4] M. J. Carlotto, "Detection and analysis of change in remotely sensed imagery with application to wide area surveillance," *IEEE Trans. Image Process.*, vol. 6, no. 1, pp. 189–202, Jan. 1997.

[5] K. R. Merril and L. Jiajun, "A comparison of four algorithms for change detection in an urban Environ.," *Remote Sens. Environ.*, vol. 63, no. 2, pp. 95–100, Feb. 1998.

[6] S. Ghosh, L. Bruzzone, S. Patra, F. Bovolo, and A. Ghosh, "A context-sensitive technique for unsupervised change detection based on hopfield-type neural networks," *IEEE Trans. Geosci. Remote Sens.*, vol. 45, no. 3, pp. 778–789, Mar. 2007.

[7] R. J. Radke, O. Andra, S. Al-Kofahi, and B. Roysam, "Image change detection algorithms: A systematic survey," *IEEE Trans. Image Process.*, vol. 14, no. 3, pp. 294–307, Mar. 2005.

[8] T. Fung and E. LeDrew, "The determination of optimal threshold level for change detection using various accuracy indices," *Photogram. Eng. Remote Sens.*, vol. 54, no. 10, pp. 1449–1454, 1988.

[9] F. Bovolo, L. Bruzzone, and M. Marconcini, "A fuzzy-statistics-based affinity propagation technique for clustering in multispectral images," *IEEE Trans. Geosci. Remote Sens.*, vol. 46, no. 7, pp. 2647–2659, Jul. 2008.

[10] A. Rosenfeld and A. C. Kak, *Digital Picture Processing*. New York, NY, USA: Academic, 1982.

[11] A. Ghosh, B. N. Subudhi, and S. Ghosh, "Object detection from videos captured by moving camera by fuzzy edge incorporated Markov Random Field and local histogram matching," *IEEE Trans. Circuits Syst. Video Technol.*, vol. 22, no. 8, pp. 1127–1135, Aug. 2012.

[12] S. Z. Li, *Markov Random Field Modeling in Image Analysis*. New York: NY, USA: Springer-Verlag, 2001.

[13] L. Bruzzone and D. F. Prieto, "Automatic analysis of the difference image for unsupervised change detection," *IEEE Trans. Geosci. Remote Sens.*, vol. 38, no. 3, pp. 1171–1182, May 2000.

[14] A. Ghosh, N. R. Pal, and S. K. Pal, "Image segmentation using a neural network," *Biol. Cybern.*, vol. 66, no. 2, pp. 151–158, Dec. 1991.

[15] J. J. Hopfield, "Neurons with graded response have collective computational properties like those of two state neurons," *Proc. Nat. Acad. Sci.*, vol. 81, no. 10, pp. 3088–3092, May 1984.

[16] Y. Bazi, F. Melgani, and H. Al-Sharari, "Unsupervised change detection in multispectral remotely sensed imagery with level set methods," *IEEE Trans. Geosci. Remote Sens.*, vol. 48, no. 8, pp. 3178–3187, Aug. 2010.

[17] G. Camps-Valls, L. Gomez-Chova, J. Munoz-Mari, J. Rojo-Alvarez, and M. Martinez-Ramon, "Kernel-based framework for multitemporal and multisource remote Sensing data classification and change detection," *IEEE Trans. Geosci. Remote Sens.*, vol. 46, no. 6, pp. 1822–1835, Jun. 2008.

[18] D. Liu, Z. Jiang, and H. Feng, "A novel fuzzy classification entropy approach to image thresholding," *Pattern Recognit. Lett.*, vol. 27, no. 16, pp. 1968–1975, Dec. 2006.

[19] R. Szeliski, R. Zabih, D. Scharstein, O. Veksler, V. Kolmogorov, A. Agarwala, M. Tappen, and C. Rother, "A comparative study of energy minimization methods for markov random fields with smoothness-based priors," *IEEE Trans. Pattern Anal. Mach. Intell.*, vol. 30, no. 6, pp. 1068–1080, Jun. 2008.

[20] S. K. Pal and D. Dutta Majumder, *Fuzzy Mathematical Approach to Pattern Recognition*. New York, NY, USA: Wiley, 1986.

[21] D. Lu, P. Mausel, E. Brondízio, and E. Moran, "Change detection techniques," *Int. J. Remote Sens.*, vol. 25, no. 12, pp. 2365–2401, May 2004.

[22] S. Patra, "Unsupervised change detection of remotely sensed images: A neural approach," Ph.D. dissertation, Dept. Comput. Sci. Eng., Jadavpur Univ., Kolkata, India, 2008.

Ashish Ghosh (M'09) is a Professor with the Machine Intelligence Unit, Indian Statistical Institute, Kolkata, India. He has authored more than 150 research papers in internationally reputed journals and refereed conferences, and has edited eight books. His current research interests include pattern recognition and machine learning, data mining, image analysis, remotely sensed image analysis, video image analysis, soft computing, fuzzy sets, neural networks, evolutionary computation, and bioinformatics. He was the recipient of the prestigious and most coveted Young Scientists Award in Engineering Sciences from the Indian National Science Academy in 1995, and computer science from the Indian Science Congress Association in 1992. He was selected as an Associate of the Indian Academy of Sciences, Bangalore, India, in 1997. He is a member of the founding team that established the National Center for Soft Computing Research at the Indian Statistical Institute, Kolkata, in 2004, with funding from the Department of Science and Technology, Government of India, and is currently the In-charge of the Center. He is acting as a member of the editorial boards of various international journals.

Badri Narayan Subudhi (S'07) received the B.E. degree in electronics and telecommunication from the Biju Patnaik University of Technology, Rourkela, India, in 2004, and the M.Tech. degree in electronics and system communication from the National Institute of Technology, Rourkela, in 2009. He is currently a Research Scholar with the Machine Intelligence Unit, Indian Statistical Institute, Kolkata, India, with financial support from Council of Scientific and Industrial Research (CSIR) scheme. He was a Visiting Scientist with the University of Trento, Trento, Italy, from 2010 to 2011. His current research interests include video processing, image processing, machine learning, pattern recognition, and remote sensing image analysis.

Lorenzo Bruzzone (S'95–M'98–SM'03–F'10) is a Full Professor of telecommunications with the University of Trento, Trento, Italy, where he teaches remote sensing, radar, pattern recognition, and electrical communications. He is the Founder and the Director of the Remote Sensing Laboratory, Department of Information Engineering and Computer Science, University of Trento. His current research interests include remote sensing, radar and SAR, signal processing, and pattern recognition. He promotes and supervises research on these topics within the frameworks of many national and international projects. He has authored or co-authored 137 scientific publications in referred international journals (93 in IEEE journals), more than 190 papers in conference proceedings, and 16 book chapters. He was invited as keynote speaker in 24 international conferences and workshops. Since 2009, he has been a member of the Administrative Committee of the IEEE Geoscience and Remote Sensing Society. He ranked first place in the Student Prize Paper Competition of the 1998 IEEE International Geoscience and Remote Sensing Symposium (Seattle, July 1998). From 1998, he was a recipient of many international and national honors and awards. He is the co-founder of the IEEE International Workshop on the Analysis of Multi-Temporal Remote-Sensing Images (MultiTemp) series. Since 2003, he has been the Chair of the SPIE Conference on Image and Signal Processing for Remote Sensing. Since 2013, he has been the Founder Editor-in-Chief of the *IEEE Geoscience and Remote Sensing Magazine*. Currently, he is an Associate Editor for the IEEE TRANSACTIONS ON GEOSCIENCE AND REMOTE SENSING. Since 2012, he has been a Distinguished Speaker of the IEEE Geoscience and Remote Sensing Society.